Available online at www.scientiaresearchlibrary.com

Scientia Research Library ISSN 2348-0416
USA CODEN: JASRHB

Journal of Applied Science And Research, 2013, 1 (1):78-89

(*http://www.scientiaresearchlibrary.com/arhcive.php*)

Monte-Carlo Simulation of positive ion transport through SF_6 plasma sheath: application to the deep silicon etching

Amand Pateau[1,2], Ahmed Rhallabi[1], Marie Claude Fernandez[1], Mohamed Boufnichel[2],Fabrice Roqueta[2]

[1] *Institut des Matériaux Jean Rouxel - Université de Nantes, 2 rue de la Houssinière 44322 Nantes - France.*

[2] *STMicroelectronics, 10, rue Thalès de Milet 37071 TOURS - France.*

ABSTRACT

Ion transport across the sheath is studied using sheath Monte-Carlo model coupled to the plasma kinetic model. The advantage of the developed simulation approach is the prediction of IEDF and IADF onto the substrate surface as a function of the operating conditions (RF power, gas pressure and flow rate). The model is applied to SF_6 ICP plasma which is widely used in material etching processes like the silicon etching. IEDF evolution at each incident angle versus SF_6 pressure is analysed. The bimodal peak due to the modulation of the DC voltage through the sheath is evidenced. The two peaks around the average energy qV_C become almost symmetric when the pressure increases. This is due to the diminution of the electron density with the pressure because of the electronegativity of SF_6 leading to the increase of the sheath thickness. The results also show the correlation between the ion mass and the width of IEDF bimodal peak. The latter is all the more wide that the ion is light. Furthermore, the simulation results show that incident energy E_i at the sheath edge strongly affects the anisotropy degree of IEDF. The latter is more anisotropic for a low E_i.

Keywords: Plasma, SF_6, Sheath, Etching, Simulation, Modelling

INTRODUCTION

Dry etching using plasma processes plays an important role in the miniaturisation of the electronic devices. Indeed, low temperature plasma discharges using the reactive gas as fluoride gas, is the most widespread process used in the material etching for semiconductor manufacturing. The existence of the sheath between the plasma, characterized by the charge quasi-neutrality, and the surface, characterized by the electronic charge depletion in comparison to the positive charges, is a major factor providing the etching anisotropy. The establishment of the vertical electric field in the sheath induces the acceleration of positive ions across the sheath and consequently the increase of their energies onto the substrate surface. The directionality of the positive ions, due to the existence of the electric field between the plasma and substrate holder, is the main factor for performing the anisotropic etching. Figure 1 illustrates an example of the deep silicon etching for integrated 3D

capacitances. The presence of one of the morphological defects along the side-wall commonly named "scalloping" is evidenced in this figure. The challenge is to perform a deep silicon etch profiles trough the masks without any morphological defect. The improving of the etching anisotropy during the pattern transfer under reactive plasmas is tributary on the knowledge of the positive ion transport phenomena across the sheath.

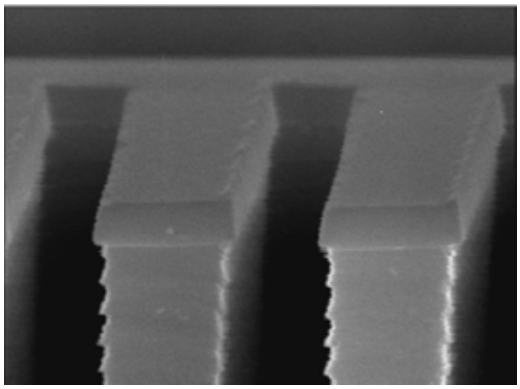

Fig 1. Silicon etching by plasma bosch process SF_6/C_4F_8.

The main parameters playing an important role in the morphological properties of micronic and submicronic etch structures are the ion energy distribution function (IEDF) and ion angular distribution function (IADF). The control of the width of such distributions especially near the surface substrate, allows the improve of the etching anisotropy. In capacitive coupled plasmas or high density plasma (HDP), IEDF and IADF depend on several parameters such as the sheath thickness, which is function of the gas pressure, electron density and temperature and DC bias [1]. For example, at low pressure, the ion/neutral collisions are less probable in the sheath leading to the peak narrowing around *0* degree at the substrate and consequently to the improvement of the etching anisotropy. Also, electron density and temperature are the main parameters controlling the average sheath thickness. The latter is all the more lower that the electron density is higher and the electron temperature is lower [2, 3]. These plasma parameters are directly affected by the operating conditions of plasma reactors such as pressure, radio frequency (RF) power, gas flow rate and reactor geometry. In high density plasmas (HDP) as Inductively Coupled Plasmas (ICP) which are widely used in etching processes, the power reactive plasma is generated by the RF source power supplied to the reactive gas. Another source power is applied to the substrate holder to control the average positive ion energy independently to the other plasma parameters. However, the physical and geometrical characteristics of the sheath located between the plasma and the substrate are still affected by the plasma parameters. As mentioned above, the sheath thickness which is a function of electron density and temperature involves the control of ion transit time across the sheath and consequently the shape of IEDF and IADF onto the substrate. Indeed, if the ion transit time across the sheath is short compared to the RF period, the ion energy corresponds to the sheath voltage at the moment it reaches the sheath edge. For a long ion transit time compared to the RF period, the ion energy more closely corresponds to the average sheath voltage [4].

In HDP plasmas and in the case of a collision-less sheath (lower pressure), IEDF is typically bimodal due to the time modulation of voltage applied to the substrate holder. The bimodal peak is related to the excitation frequency and ion mass [5]. The measurement of IEDF and IADF is still, until now, difficult especially near the substrate holder. Nevertheless, several experimental studies

dedicated to the determination of IEDF and IADF have been achieved [6] but few of these experimental works have given information about both IEDF and IADF at the substrate holder.
The calculation of IEDF and IADF using a simulation requires the development of a self-consistent simulation approach including electromagnetic, and neutral/charge kinetic phenomena [7]. This can be done using Particle In Cell method or fluid method coupled to Monte-Carlo method [8, 9]. Such modelling approaches are still difficult to develop and are time consuming. Beside, sheath models in RF plasma discharge, based on the use of an effective electric field applied to the positive ions, have been developed [10, 11].
Furthermore, hybrid methods using multi-scale approaches including both plasma kinetic model based on global model, sheath model and also 2D or 3D etching models [2, 3, 12] have been developed. This approach is applied to the etching of silica [3] and InP [12] materials.
In this study, we have developed a sheath model based on the Monte-Carlo method to study the positive ion transport phenomena across the sheath located between plasma and substrate. Even if the model is not consistent, its advantage is its ability to estimate IEDF and IADF of SF_6 plasma in a reasonable simulation time.
In section II, we present a brief description of the plasma kinetic model which was already developed in our previous work [13]. In a second time, we present the sheath model based on the Monte-Carlo method by commenting some hypothesis involved in this study. In section III, we present some simulation results from plasma kinetic model which are used as input parameters in sheath model and in a second time, we focus our study on the analysis of sheath simulation results in terms of IEDF and IADF for SF_6 plasma discharge. A conclusion is presented in section IV.

MATERIALS AND METHODS

MODEL

Figure 2 presents the flowchart of our modelling approach. It is composed of two modules permitting the calculation of IEDF and IADF as a function of plasma parameters. The first module consists in the plasma kinetic model of SF_6 based on the zero dimensional (*0*D) global model [13]. It enables the calculation of average densities and fluxes of neutral and ions as well as the electron density and temperature. Such parameters are used as input parameters in the sheath model. The second module consists in the sheath model which allows the study of the ion transport across the sheath using Monte-Carlo method. The output data of the model are IEDF and IADF.

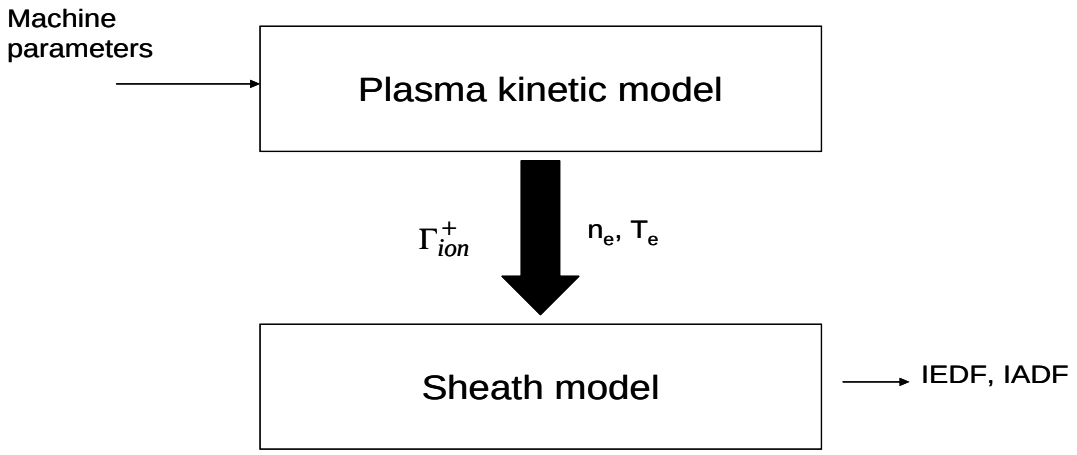

Fig 2. Model flowchart.

A. Plasma kinetic model

Details of the plasma kinetic model of SF_6 are presented in [13]. *0*D global approach is applied, which consists in the calculation of the average densities and fluxes of neutral and ion species taken into account in the reaction scheme. The simulations are performed considering an inductively coupled plasma (ICP) with cylindrical geometry. Mass balance equations associated to neutral and ion species coupled to charge neutrality equation and power balance equation allow the calculation of neutral and ion densities as well as the electronic density and temperature [12_15].

9 neutral species SF_x (x = 0 - 6), F_y ($y = 1, 2$), 7 negative ions SF_y^- ($y = 2 - 6$) and F_z^- (z = 1, 2), and 7 positive ions SF_w^+ (w = 0 - 5) and F^+. The establishment of mass and power balance equations is based on a set of reaction scheme composed of 62 reactions. The rate coefficients of electronic impact reactions are deduced from [15-22]; the rate coefficients of neutral/neutral, ion/neutral and ion/ion reactions are deduced from [23]. The surface loss or production rate coefficients are calculated using Chantry theory [24] while the positive ion loss coefficients are deduced from [15]. The solving of the differential non linear equation system is performed from $t = 0$ until reaching the steady state when all neutral and ions densities as well as the electron density and temperature become independent of time. At $t = 0$, all the neutral and ion densities are set equal to zero except the primary precursors SF_6 which initial densities are given as:

$$n_i = N_o,\ i = SF_6 \tag{1}$$

where N_o is the initial total density calculated by considering perfect gas law $N_o = \frac{P}{K \times T_g}$, where P is the gas pressure, T_g is the gas temperature and K is the Boltzmann constant. To start the numerical solving of the system, we set an arbitrary value of n_e and T_e at $t = 0$. In our case, we set low values of n_e, typically $n_e = 10^7 cm^{-3}$, and $T_e = 3\ eV$. To respect the charge neutrality at $t = 0$, we set $n_{SF^+} = n_e$.

Among the output data from SF_6 global model are the positive ion fluxes which are used as input parameters in the sheath model. The positive ion fluxes are determined as:

$$\Gamma_i^+ = n_i^+ \times u_i^+ \tag{2}$$

where n_i^+ is the ion density of species i and u_i^+ is the Bohm velocity. The latter is determined as:

$$u_i^+ = \sqrt{\frac{q\,T_e\,(1+\alpha)}{M_{+,i}\,(1+\gamma\alpha)}} \tag{3}$$

where q is electron charge, T_e is the electron temperature, $M_{+,i}$ is the ion mass, γ is the ratio of the electron temperature to the negative ion temperature and α is the ration of negative ion density to electron density. According to the equation (3), the electronegativity of plasma discharge, which can be quantified by the parameter α, affects the positive ion velocity at the edge of the sheath. Bohm velocity decreases with α.

B. Sheath model

In general, the calculation of IEDF and IADF as a function of operating conditions requires the development of self-consistent particular approaches such as Particle In Cell - Monte Carlo Collision (PIC - MCC) [8, 9]. This method consists in the solving of the Maxwell equations coupled to the transport of electrons, ions and, in certain cases, neutral species in 2D or 3D. Obviously, the

method gives more accurate results. However, it is very hard to achieve and time consuming. The advantage of our alternative approach that we have developed is its a low time consuming even if we use a complex plasma mixture like SF_6 containing several positive ion species. The main idea of this method is to consider a semi empirical axial profile of the electric field along the sheath containing parameters that would be fit according to operating conditions. This avoids, in each compute time step, the solving of Poisson equation across the sheath to deduce the voltage profile and consequently the electric field which is an essential parameter to solve the Newton equation required for the positive ion displacement. So the electric sheath equation is given as:

$$E(z,t)=V_{cs}\frac{n}{d}\left(\frac{z}{d}\right)^{n-1} \tag{4}$$

where *E(z,t)* is the electric field, *z* is the axial coordinate (*z = 0* at the sheath edge), *n* is constant between *0.5* and *1* [1]. The value of *n* is a function of d/λ^{++} (with λ^{+} the total ion mean free path, including all collision processes). In our simulations, *n* is fixed at *0.75*. The sheath thickness was calculated by using data given by the kinetic model using collisionless Child-Langmuir model.

$$d=\lambda_D\left(\frac{qV_c}{T_e}\right)^{3/4} \tag{5}$$

where λ_D is the the Deby length which is determined as a function of n_e and T_e deduced from the kinetic model:

$$\lambda_D=\left(\frac{\varepsilon T_e}{q^2 n_e}\right)^{1/2} \tag{6}$$

V_c is the voltage between the substrate holder and the sheath edge. The time evolution of the voltage through the sheath is given as:

$$V_{cs}(t)=V_c\left[1+\Omega\sin(2\pi f_{RF}\,t)\right] \tag{7}$$

which $\Omega=\frac{V_a}{V_c}$. V_a is the RF amplitude of the sheath voltage and f_{RF} is the RF frequency which is fixed at *13.56 MHz*. For our simulations, $\Omega=0.9$. Indeed, Manenschijn et al. have measured V_c and V_a voltages as a function of power in capacitance reactor [1]. At low power, Ω is almost equal to *1* and decreases at higher power to reach 0.75.

The flowchart of the Monte-Carlo sheath model is summarised as follow: the ion type is selected randomly according to its fraction. After that, it is placed at the edge of the sheath (*z = 0*) while their *(x, y)* coordinates are randomly selected. Time *t* is randomly selected between *0* and RF period t_{RF} . At each time step, the ion is moved by solving the Newton equation:

$$m_i^{ion}\frac{d\,\vec{v}_i^{ion}}{dt}=q\,\vec{E}(z,t) \tag{8}$$

where m_i^{ion} and $\vec{v}_i^{ion}$ are the ion mass and velocity respectively. The ions are moved until reaching *z = d* corresponding to the substrate surface; then their energy and incident angle are stored. The programme is looped until the fixed ion number. For our simulation, the ion number is

10^6. The storage of all ion angles and energies allows the calculation of IEDF and IADF. We note that in our Monte-Carlo model, ion neutral collisions in the sheath are neglected because of the high free path of ions comparing to the sheath thickness.

RESULTS AND DISCUSSIONS

As mentioned above, some input parameters of the sheath model as sheath thickness and positive percentage are deduced from the plasma kinetic model. The calculation of sheath thickness is estimated as a function of n_e and T_e using collisionless Child-Langmuir model [3, 12].

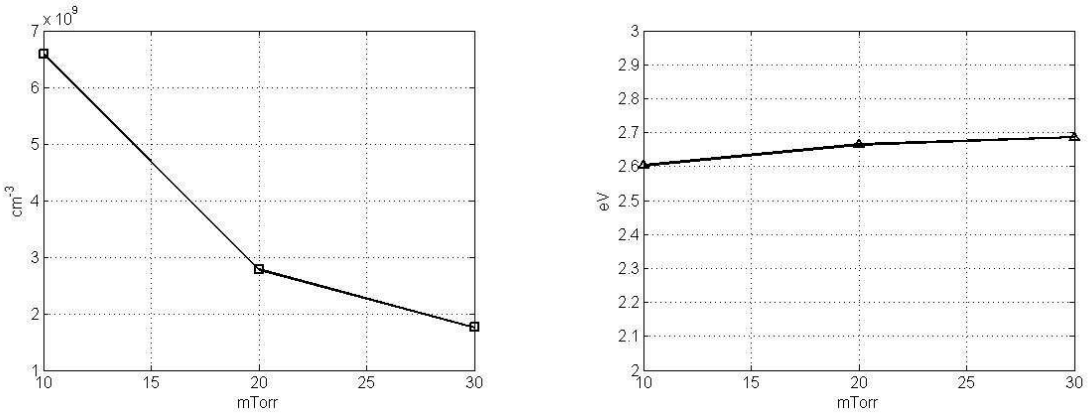

(a) (b)

Fig 3. Variation of n_e (a) and T_e (b) with pressure values, P_{RF} *= 1500 Watt, Q(SF6) = 200 sccm.*

Figure 3 shows n_e and T_e evolution with pressure for P_{RF} *= 1500 Watt* and $Q(SF_6)$ *= 200 sccm*. In this RF pressure conditions, a slight increase of T_e is observed while n_e strongly decreases with the pressure. This is due to the high electro-negativity of SF_6 gas. The electronic attachment processes are all the more favoured that the pressure is higher. These parameters directly affect the sheath thickness. Indeed, according to the equations (5 ,6), $d \propto T_e^{-1/4}\, n_e^{-1/2}\, V_c^{3/4}$. In our pressure range, T_e is almost constant; so these are the diminution of n_e and the increase of V_c that cause the enhancement of d with the pressure (Fig. 4).

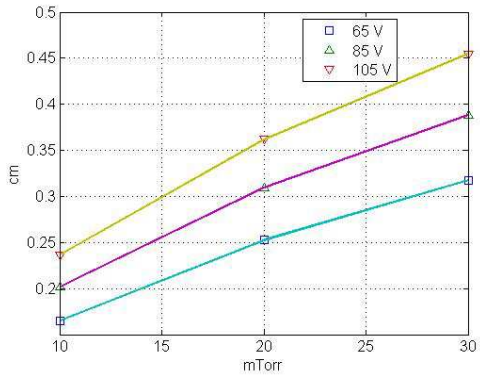

Fig4. Sheath thickness versus gas pressure for different V_c values; P_{RF} *= 1500 Watt,* $Q(SF_6)$ *= 200 sccm.*

Another input parameters estimated from the plasma kinetic model which are useful for the sheath model are the positive ion flux percentages. Figure 5 displays the positive ion flux percentage variation with the pressure for P_{RF} *= 1500 Watt* and $Q(SF_6)$ *= 200 sccm*. At low pressure, SF_5^+ is the dominant positive ion which tends to decrease with the pressure. Over *20 mTorr*, SF_3^+ becomes the dominant positive ion. We also observe that both F^+ and SF_4^+ flux percentages decrease with the pressure but they are still *2* to *8* times lower than those of SF_5^+ and SF_3^+. Noting that the percentages of SF^+, SF_2^+, S^+ and F_2^+ are lower than *1%*.

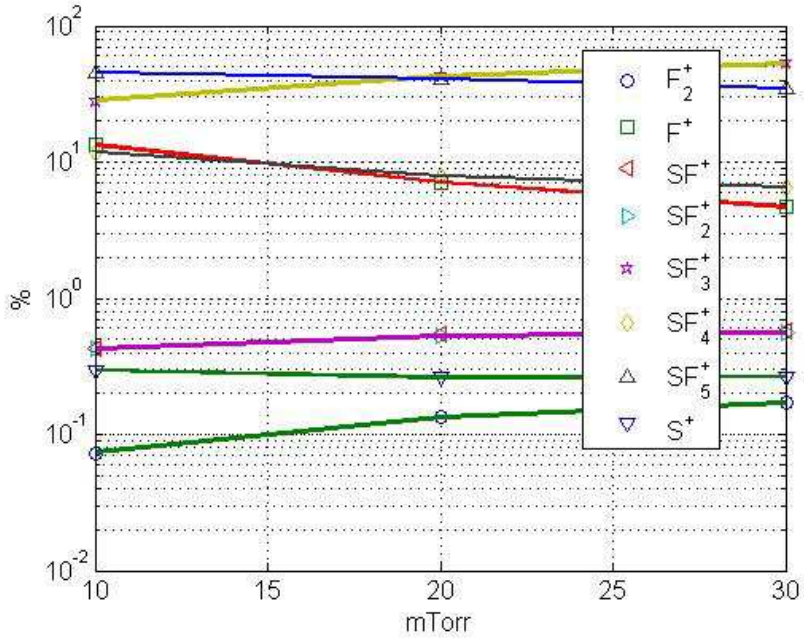

Fig 5. Ion percentage versus gas pressure for P_{RF} *= 1500 Watt,* $Q(SF_6)$ *= 200 sccm*

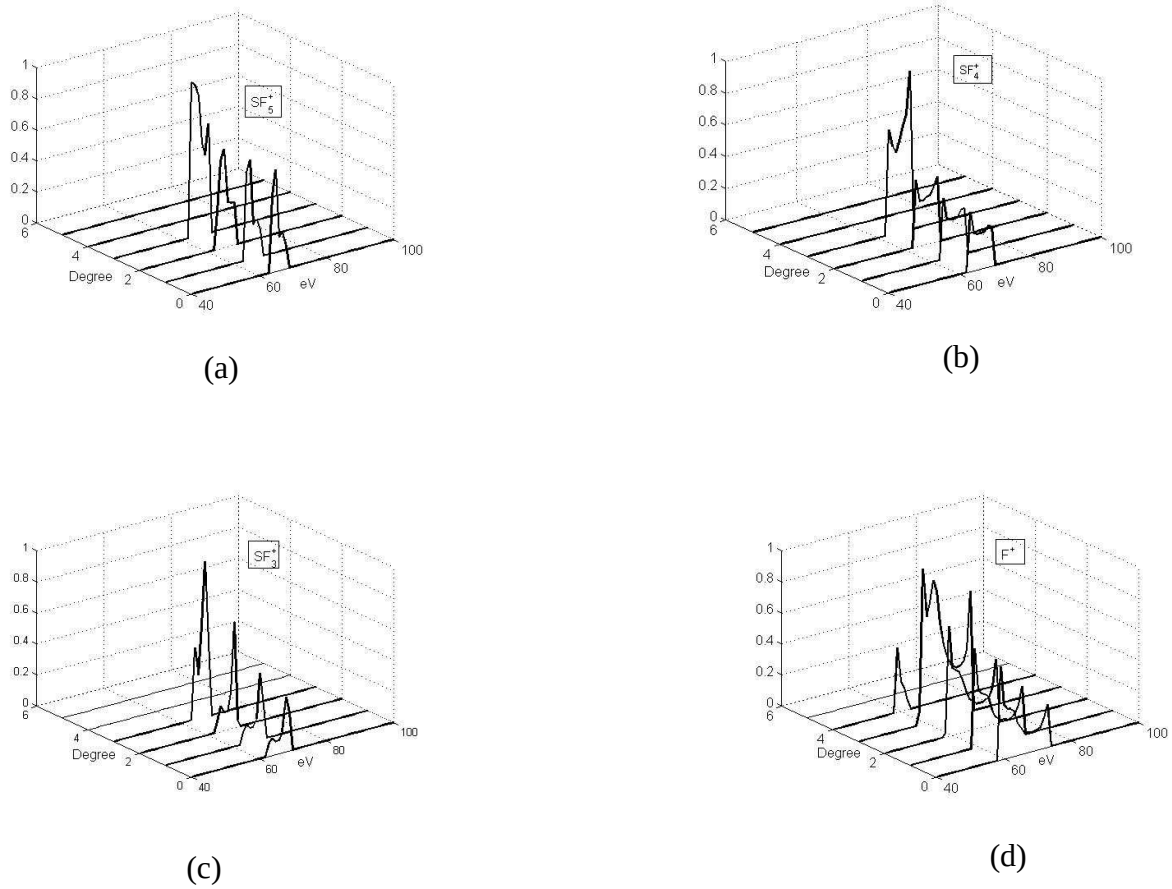

Fig 6. IEDF at each ion incident angle *for p = 10 mTorr, P_{RF} = 1500 Watt, $Q(SF_6)$ = 200 sccm.*

Figure 6 presents the IEDF versus the ion incident angle determined at *p = 10 mTorr*, P_{RF} = *1500 watt* and $Q(SF_6)$ *= 200 sccm*. In these operating conditions of SF_6 plasma, $n_e = 6.59\ 10^9$ cm^{-3} and $T_e = 2.6\ eV$. From these values and $V_c = 65\ V$, the sheath thickness $d = 0.16\ cm$. SF_5^+ , SF_4^+ , SF_3^+ and F^+ are the dominant positive ions. For all considered ions, IEDFs are bimodal and centred around $q\ V_c = 65\ eV$. At *30 mTorr* pressure (Fig. 7), the sheath thickness $d = 0.32\ cm$ is calculated for $n_e = 1.75\ 10^9$ *mTorr* and $T_e = 2.68\ eV$ determined from the plasma kinetic model. In these conditions, the widths of the bimodal IEDFs narrow in comparison to those at *10 mTorr*. The increase of the pressure leads to the increase of the sheath thickness. The presence of two major peaks is due to the modulation of the voltage V_{cs} across the sheath. At *30 mTorr* pressure, the two peaks around $q\ V_c$ are almost symmetric whereas at *10 mTorr* we observe a strong asymmetry of the peaks especially for SF_3^+ species. Indeed, at *30 mTorr*, the electric field is less important because of the high sheath thickness in comparison with that at *10 mTorr* (Fig. 8).

The time transit of ions are all the more important that the ions have much time to move across the sheath and oscillate along the electric field. Furthermore, we can observe that the IEDF peak is more important at *3 degree* ion incident angle and disappears for angles higher than *3 degree*. Such IEDF behaviour is already observed in [25]. On the other hand, In both *10 mTorr* and *30 mTorr*, the IEDF bimodal peaks are all the more wide that the ion mass is low.

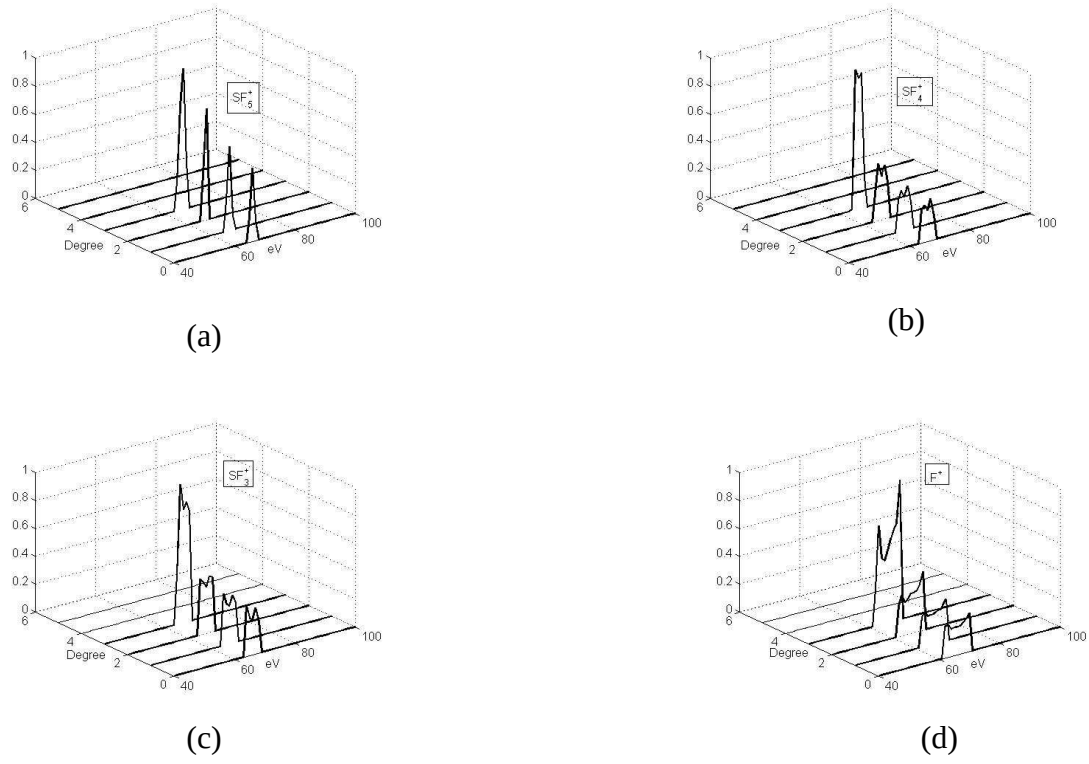

Fig 7. IEDF at each ion incident angle for *p = 30 mTorr*, *PRF = 1500 Watt, Q(SF6) = 200 sccm*.

The time transit of ions are all the more important that the ions have much time to move across the sheath and oscillate along the electric field. Furthermore, we can observe that the IEDF peak is more important at *3 degree* ion incident angle and disappears for angles higher than *3 degree*. Such IEDF behaviour is already observed in [25]. On the other hand, In both *10 mTorr* and *30 mTorr*, the IEDF bimodal peaks are all the more wide that the ion mass is low.

Figure 9 shows the effect of ion incident energy E_i at the sheath edge on IEDF versus angle considering as example SF_5^+ and SF_4^+. As seen in figures 6,7 which the simulation results are given for $E_i = 0.3\ eV$, the main bimodal peak is located at *3 degree* of incident angle. In these conditions, the ions arriving at the edge of the sheath with a high incident angle have not much time to orient along the axial direction *z* of electric field. A significant part of this ion population reaches the substrate surface with angle greater than *0*. However, when the ions reach the sheath edge with $E_i = 0.026\ eV$ (low incident energy), the main bimodal peak of IEDF is located at *0* degree of incident ion leading to a high anisotropy of IEDF. Such parametric study reveals that the knowledge of the incident ion energy E_i is very important to predict the IEDF shape.

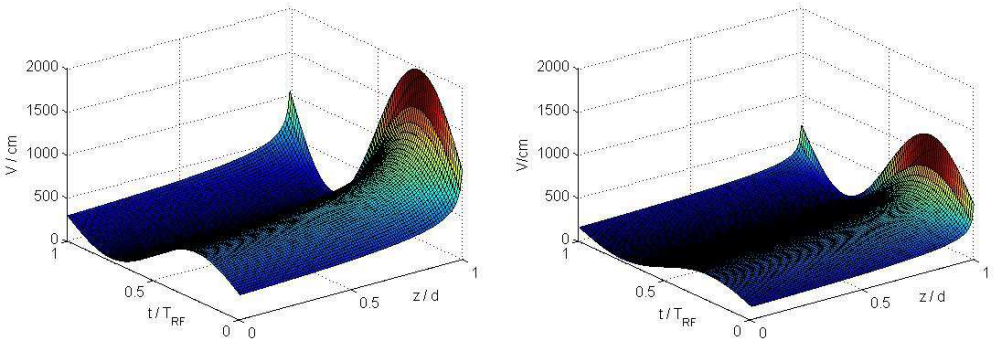

(a) (b)

Fig 8. Electric field profile versus t/T_{RF} and $z = d$ for $p = 10$ *mTorr* (a), $p = 30$ *mTorr* (b), $P_{RF} = 1500$ *Watt* and $Q(SF_6) = 200$ *sccm*.

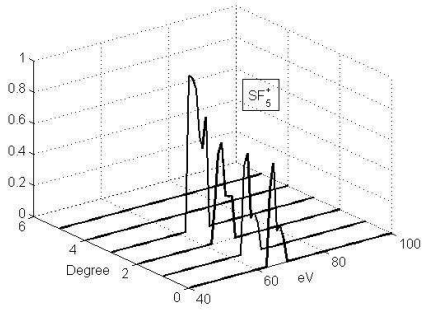

(a) $E_i = 0.3$ *eV*

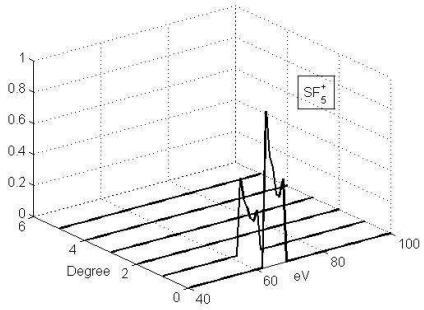

(b) $E_i = 0.026$ *eV*

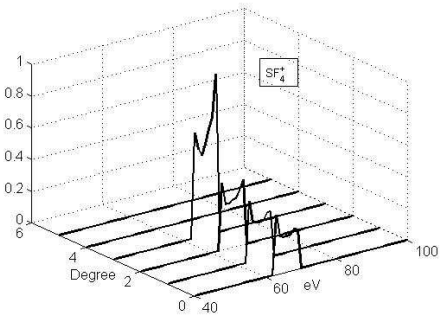

(c) $E_i = 0.3$ *eV*

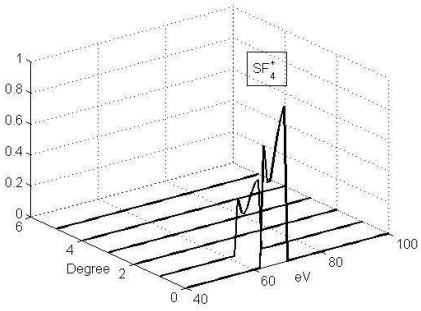

(c) $E_i = 0.026$ *eV*

Fig 9. Effect of the initial ion energy E_i at the sheath edge on the IEDF for $p = 10$ *mTorr*, $P_{RF} = 1500$ *Watt*, $Q(SF_6) = 200$ *sccm*.

CONCLUSION

Plasma kinetic model of SF_6 coupled to the sheath model is developed to predict the ion properties into the substrate surface. This is useful to analyse the etch profile through the mask and the etch rate evolution. The plasma kinetic model based on *0D* global approach allows the calculation of the ion fluxes as well as the electron density and temperature. These parameters are introduced as input parameters in the sheath model to evaluate the sheath thickness and the fraction of the ion population. The advantage of this simulator is the prediction of IEDF at each incident angle as a function of the operating conditions of ICP reactor. The effect of the pressure in pure SF_6 plasma on the IEDF is analysed. The simulation results reveal that for electronegative gas as SF_6, the electron density decreases with the pressure because of the increase of the electronic attachment processes. This leads to the increase of the sheath thickness which involves more symmetrical bimodal peaks around $q\ V_c$. Furthermore, the simulation results show that the incident ion energy E_i plays an important role in the IEDF anisotropy evolution. IEDF is all the more anisotropic that E_i is low.

ACKNOWLEDGEMENTS

This study is financially supported by STMicroelectronics Tours - France.

REFERENCES

[1] A. Manenschijn, G. C. A. M. Janssen, E. van der Drift, and S. Radelaar, Journal of Applied Physics, **1991**, 69, 1253.
[2] G. Marcos, A. Rhallabi, and P. Ranson, J. Vac. Sci. Technol. **2004**, B 22, 1912.
[3] L. Lallement, A. Rhallabi, C. Cardinaud, and M. Fernandez, J. Vac. Sci. Technol. **2011**, A 29, 051304.
[4] S. B. Wang and A. E. Wendt, J. Appl. Phys. 200, 88, 643.
[5] W. M. Holber and J. Forster, J. Vac. Sci. Technol. **1990**, A 8, 3720.
[6] J. Zheng, R. P. Brinkmann, and P. M. James Vittie, J. Vac. Sci. Technol. **1995**, A13, 859.
[7] P. L. G. Ventzek, R. J. Hoekstra, and M. J. Kushner, J. Vac. Sci. Technol. **1994**, B 12, 461.
[8] C. K. Birdsall, IEEE Trans. Plasma Sci. **1990**, 41, 1112.
[9] V. Vahedi and M. Surendra, Comp. Phys. Comm. **1995**, 87, 179.
[10] P. A. Miller and M. E. Riley, J. Appl. Phys. **1997**, 82, 3689.
[11] T. Panagopoulos and D. J. Economou, J. Appl. Phys. **1999**, 85, 3435.
[12] R. Chanson, A. Rhallabi, M. C. Fernandez, C. Cardinaud, S. Bouchoule, L. Gatilova, and A. Talneau, IEEE Trans. Plasma Sci. **2012**, 40, 959.
[13] L. Lallement, A. Rhallabi, C. Cardinaud, M. Peignon-Fernandez, and L. Alves, Plasma Sources Sci. Technol. **2009**, 18, 025001.
[14] A. Rhallabi and Y. Catherine, IEEE Trans. on Plasma Sci. **1991**, 19, 270.
[15] C. Lee and M. Lieberman, J. Vac. Sci. Technol. **1995**, 13, 368.
[16] L. Christophorou and J. Oltho_, J. Phys. Chem. Ref. Data, **2000**, 29, 267.
[17] M. Ito, M. Goto, H. Toyoda, and H. Sugai, Contrib. Plasma Phys. **1995**, 35, 405.
[18] J. Gudmundsson, J. Phys. D: Appl. Phys. **2002**, 35, 328.
[19] M. Lieberman and R. Gottscho, Physics of Thin Films, New York Academic Press, **1994**.
[20] V. Tarnovsky, H. Deutsch, K. Martus, and K. Becker, J. Chem. Phys. **1998**, 109, 6596.
[21] R. Freund, R. Wetzel, R. Shul, and T. Hayes, Phys. Rev. A , **1990**, 41, 3575.

[22] K. Hosomi, T. Kikawa, S. Goto, H. Yamada, T. Katsuyama, and Y. Arakawa, J. Vac. Sci. Technol. **2006**, B 24, 1226.
[23] K. Ryan and I. Plumb, Plasma Chem. Plasma Process. **1990**, 10, 207.
[24] P. Chantry, J. Appl. Phys. **1987,** 62, 1141.
[25] A. D. Huypers and H. J. Hopman, J. Appl. Phys. **1990**, 67, 1229.